cross-linking by vinyl polymerization with some hydrosilylation at low temperatures, extensive Si-Si, C-H, and Si-H bond cleavage with radical formation and methylene insertion at intermediate temperatures, and finally consolidation of the "SiC" network, along with the formation of free carbon and partial crystallization of the ceramic product at higher temperatures. ^{1}H, ^{13}C, and ^{29}Si MAS NMR reveal structural details of the polymer-to-ceramic conversion that are unavailable by typical XRD techniques and give insight into the chemical bonding and phase composition of these inorganic amorphous polymers.

The application of solid-state NMR, along with other analytical methods, has provided an improved understanding of the chemical decomposition of a commonly used vinylic polysilane precursor to ceramic SiC. This information should assist in designing new ceramic precursors to meet specific processing objectives, such as the enhancement of ceramic yield and the production of innocuous byproducts, or with tailorable physical properties, such as solubility and viscosity, for preparation of thin films or continuous fiber.

Acknowledgment. We acknowledge the support of the National Science Foundation under Materials Chemistry Initiative Grant No. CHE-8706131 and the Colorado State University Regional NMR Center, funded by NSF Grant No. CHE-8616437. C. E. Bronnimann provided invaluable assistance in obtaining CRAMPS spectra. W.R.S. acknowledges Dr. G. M. Renlund at General Electric Corporate Research and Development for assistance with TGA/DTA experiments, Mr. W. Hurley, Jr., for assistance with isolation of preceramic materials and determination of the proposed composition of the vinylic polysilane, Mr. C. Warren for preliminary analyses of decomposition gases, and Mr. C. Whitmarsh for insightful NMR discussions. Dr. C. L. Czekaj is thanked for solution NMR experiments. Mr. R. Lewis is acknowledged for ESR experimental work.

Registry No. SiC, 409-21-2.

Loss of Halide from Sol-Gel Films on Heating Does Not Involve Oxidation[1]

Carol L. Schutte[†,‡] and George M. Whitesides*[,†]

Department of Chemistry, Harvard University, Cambridge, Massachusetts 02138, and Department of Materials Science and Engineering, Massachusetts Institute of Technology, Cambridge, Massachusetts 02139

Received July 11, 1990. Revised Manuscript Received December 5, 1990

The loss of halide ion from sol-gel-derived films on heating has been studied by Rutherford backscattering spectrometry. The rates of loss of halide under air and argon atmospheres were very similar. This observation is consistent with a nonoxidative mechanism for the loss of halide. The relative rate of loss of halide at a particular temperature follows the qualitative order LiI > LiBr ≃ LiCl > NaI > NaBr > KI ≃ KBr ≃ NaCl. This order correlates with the vapor pressures of the salts and with the ΔG of formation of the hydrogen halides by reaction of metal halide with water and suggests that volatilization of the salt and/or the hydrogen halide is the mechanism for loss of halide ion from sol-gel coatings.

Introduction

Hydrogen halides and halide salts are catalysts used in sol-gel reactions to affect the time required for gelation.[2,3] Chlorine gas dehydroxylates surface silanols in sol-gel-derived glass during sintering. This reduction in OH content avoids bubbling or foaming of the glass on further heating.[4] Little is known about the fate of the ions after gelation or sintering, although the halides are known to disappear from the gel during its transformation to glass at high temperatures. The goal of this study was to investigate the mechanism of loss of halide ion from sol-gel coatings on heating. We have used Rutherford backscattering spectrometry (RBS) to quantify the content of halide ion (and non-halogen anions) in silica films derived from sol-gels as a function of the temperature and atmospheres under which they were heated. We have also used Auger electron spectroscopy (AES) for qualitative analysis for the presence of sodium in a NaI-doped SiO_2 sample both before and after thermal treatment.

Mechanisms for the Loss of Halide in Sol-Gel Coatings. Halogen could, in principle, be lost from the silica film either as HX or M^+X^- or, following oxidation, as X_2 (eqs 1-4; Si_l denotes a representative silicon center volatilization of HX:

$$Na^+X^- + HOSi \rightarrow HX\uparrow + NaOSi_l \quad (1)$$

$$Na^+X^- + HOH \rightarrow HX\uparrow + NaOH \text{ (or } Na_2O) \quad (2)$$

volatilization of MX:

$$Na^+X^- \rightarrow Na^+X^-\uparrow \quad (3)$$

oxidation of X^- to X_2:

$$2Na^+X^- + \tfrac{1}{2}O_2 \rightarrow X_2\uparrow + Na_2O \quad (4)$$

in the silicate lattice). It is possible that mass transport of some species (M^+X^-, HX, X^-, X_2, O_2, H_2O) might be rate-limiting. The only plausible oxidant under normal

[†] Harvard University.
[‡] Massachusetts Institute of Technology.

(1) Supported in part by the National Science Foundation (CHE-88-12709), the Office of Naval Research, and the Defense Advanced Research Projects Agency (through the University Research Initiative). The Cambridge Accelerator for Materials Science was purchased through a DARPA/URI grant and is housed in the Harvard University Materials Research Laboratory, an NSF-funded facility (DMR-86-14003).

(2) Pope, E. J. A.; Mackenzie, J. D. *J. Non-Cryst. Solids* **1986**, *87*, 185-198.

(3) Melpolder, S. M.; Coltrain, B. K.; Salva, J. M. In *Proceedings of the Fourth International Conferences on Ultrastructure Processing of Ceramics, Glasses, and Composites, Tucson, Arizona, February, 1989*; Uhlmann, D. R., Ulrich, D., Eds., to be published.

(4) Shin Satoh, I.; et al. U.S. Patent 4,426,216, Jan 1984.

0897-4756/91/2803-0267$02.50/0

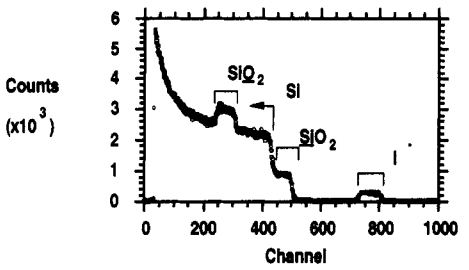

Figure 1. Representative RBS spectrum obtained for a coating of LiI-doped SiO_2 on a silicon substrate.

conditions for thermal transformation of gel to glass is atmospheric oxygen. It should, therefore, be possible to distinguish between mechanisms for loss of halide on heating by examining the rates of loss of anion from the gel for anions differing in the volatility of their conjugate protic acids (eqs 1 and 2) and their salts (eq 3) and in their susceptibility to oxidation (eq 4).

Experimental Section

Chemicals: Sodium iodide, sodium bromide, and ammonium vanadate were purchased from Fisher Scientific Co. Tetraethylorthosilicate (TEOS), lithium iodide, lithium chloride, and hydrogen hexafluoroantimonate(V) were purchased from Alfa, and absolute ethanol was from USI Chemicals Co. Sodium chloride was purchased from Mallinckrodt. Potassium bromide and potassium iodide were purchased from Merck. Lithium bromide was purchased from Bradford Scientific, Inc. All reagents were used without purification.

RBS analysis: The depth profiles of I, V, and O were obtained by using the Cambridge Accelerator for Materials Science with a 2-MeV He^+ beam with a diameter of 1 mm. Backscattered particles were detected at 176°, relative to the incoming ion beam, with a 150-mm^2 silicon surface barrier detector placed approximately 3 in. from the sample and coupled to a multichannel analyzer. Depth profiles of I, V, and O were calculated by using the program SPECTRUM ANALYSIS,[5] as were the integrals of their signals.

Figure 1 shows a representative spectrum of a LiI-doped SiO_2 coating on a silicon substrate. The signal for iodide was at highest energy (~channels 800–730). The signal for silicon in the SiO_2 coating (~channels 500–430) was lower in intensity than for that in the substrate (~channel 430) because it was "diluted" by the other components (O, Li^+, and I^-) in the coating.

AES analysis: AES analyses were performed on a Perkin-Elmer Model 660 Auger spectrometer housed at the Center for Materials Science and Engineering and the Cambridge Surface Facility at MIT. Samples were sputtered with 2-keV argon ions (condenser lens setting 4.01; objective lens setting 3.83; ion current density 15 $\mu A/cm^2$) prior to analysis with 5-keV electrons (raster size 1.4 mm × 1.4 mm).

Hydrolysis of TEOS: A solution containing TEOS (61 mL, 273 mmol of Si), ethanol (43 mL), doubly distilled water (5 mL), and aqueous HCl (0.2 mL of 1 M acid) was heated at 60 °C for 1.5 h. After the solution was cooled to room temperature, an additional 4.0 mL of doubly distilled water and 12 mL of HCl were added to a 100-mL aliquot of the TEOS solution, and the mixture was stored in a freezer (−8 °C), where it was stable (did not gel) for several months. For coating, the solution was diluted by a factor of 3 with ethanol (0.62 mmol of Si/mL).[6]

Procedure for doping TEOS with salt: A solution of NaI in doubly distilled water (0.5 mL, 0.08 mM) was added to the previously hydrolyzed TEOS (3.10 mM of Si, 5 mL) solution. We coated the sample immediately.

Preparation of samples: We coated a silicon ⟨100⟩ wafer using a four-step procedure: first, rinsing the wafer with two 2-mL aliquots each of hexane and ethanol; second, spinning the sample dry on the spin coater (Headway) after addition of each aliquot; third, pipetting 2-mL aliquots of halide-doped TEOS solution onto the silicon substrate; fourth, spinning the substrate at 1500 rpm for 2 min. The addition of salts to the TEOS solution affected the viscosity of the solution to various degrees. Because the viscosity of the solution affects the thickness of the coating in spin-coating, the thicknesses of the coatings varied depending on which salt was added. Samples were heated in a Fisher Scientific Model 497 isotemp programmable ashing furnace at 1 °C/min, held for 3 h at the desired temperature, and cooled to room temperature at 1 °C/min. Samples were analyzed by RBS and returned to the ashing furnace for subsequent thermal treatment.

(5) SPECTRUM ANALYSIS, written by Patrick M. Smith, Division of Applied Sciences, Harvard University, is a FORTRAN program based on algorithms from: Chu, W. K.; Mayer, J. W.; Nicolet, M. A. *Backscattering Spectrometry*; Academic Press: New York, 1977.

(6) Brinker, J.; Keefer, K. D.; Schaefer, D. W.; Assink, R. A.; Kay, B. D.; Ashley, C. S. *J. Non-Cryst. Solids* **1984**, *63*, 45–59.

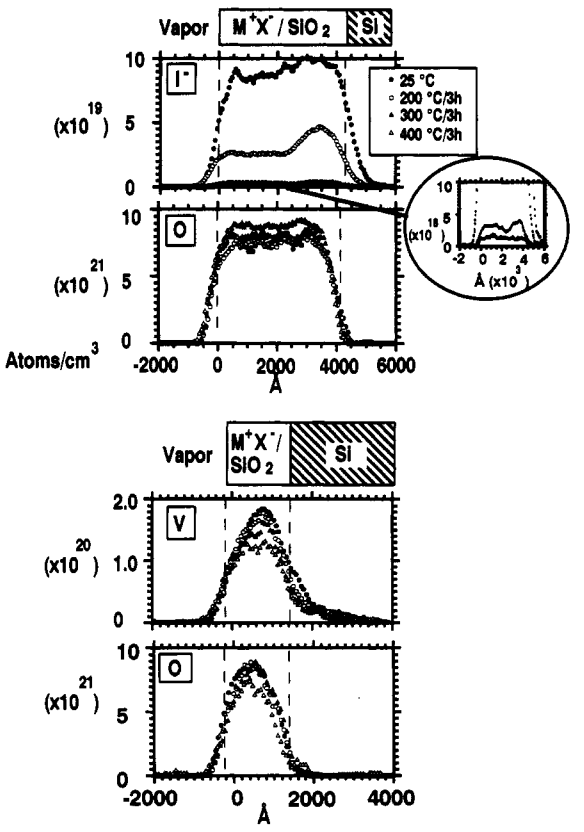

Figure 2. Representative depth profiles of iodide and oxygen from Li^+I^--doped SiO_2 and of vanadium and oxygen from $NH_4^+VO_3^-$-doped SiO_2 as a function of temperature of thermal treatment.

Results and Discussion

Procedure: We examined the mechanism of loss of halide ion experimentally by determining the quantity and distribution of anions present in silica gels as a function of thermal history and of the atmosphere (argon or air) under which they had been heated. Heating involved increasing the temperature of the sample linearly to a predetermined value, holding that temperature for 3 h, and then cooling linearly to room temperature. Multiple samples containing the same anion were subjected to one cycle of heating and cooling, analyzed for anion, and then reheated to a higher temperature, cooled, and reanalyzed.

The contents and distributions of anions in the silica gel/glass were established by RBS. Figure 2 shows representative distributions for a volatile anion (Li*I*) and for a less volatile one (NH_4VO_3) as a function of temperature of thermal treatment. Profiles for oxygen (from LiI/SiO_2 and NH_4VO_3/SiO_2) are included for comparison. The limit of depth resolution of RBS for these coatings is approximately ±200 Å.

RBS detects atoms through elastic collisions of helium ions with their nuclei. The energy of the backscattered

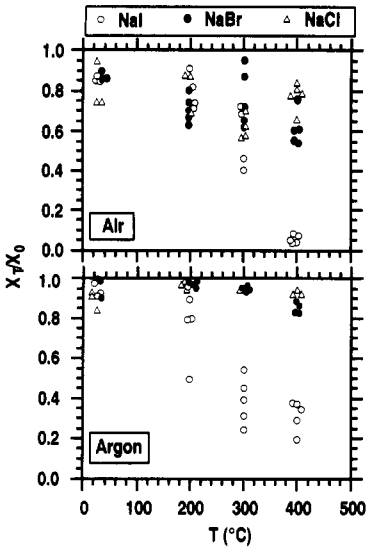

Figure 3. Plot of the normalized content of sodium halide (I^-, Br^-, and Cl^-), determined by RBS, as a function of thermal treatment (held at each temperature for 3 h) under both air and argon. Multiple points indicate measurements from multiple samples. The points are shown displaced from the nominal temperatures to avoid overlap.

helium ion and the efficiency with which it scatters are directly proportional to the atomic number of the nucleus with which it collides. RBS could not accurately measure the presence of lithium or sodium in these samples because their atomic masses are low.[7,8]

Kinetics of loss of the anion: Figure 3 summarizes data showing the relative loss of I^-, Br^-, and Cl^-, with Na^+ as counterion, as a function of temperature under argon and under air. This figure plots the normalized content of halide as a function of temperature of thermal treatment. The normalized content of halide, X_T/X_0, is the ratio of the content of halide after thermal treatment at temperature T (X_T), to the content of halide prior to thermal treatment (X_0). We measured the content of halide by calculating the ratio of the integrated areas of the halide signal to that of a predetermined region of the spectrum from the ⟨100⟩ silicon wafer substrate. We chose the silicon substrate (ρ = 2.33 g/cm^3)[9] as an internal standard.

The data in Figure 3 are scattered; nevertheless, it is clear that the content of iodide decreases faster than that of bromide or chloride. There may also be a small difference in the relative rates of loss of the halides under argon and under air, with rates apparently slightly faster under air (especially at 400 °C).

We have surveyed several anions using this technique. Results are summarized in Figure 4. The scatter in these data was similar to that in Figure 3. The individual data are omitted; the error bars represent the range of data (highest to lowest), the symbols their mean. Qualitatively, the order of disappearance of these anions is I^- (LiI) > Br^- (LiBr) ≃ Cl^- (LiCl) > I^- (KI) ≃ Br^- (KBr) ≃ SbF_6^- ($HSbF_6$) ≃ VO_3^- (NH_4VO_3). In these data, there is no significant difference in the loss of halide under air and under argon.

Figure 5 presents a plot of the temperature of the half-life for loss of halide under our experimental thermal

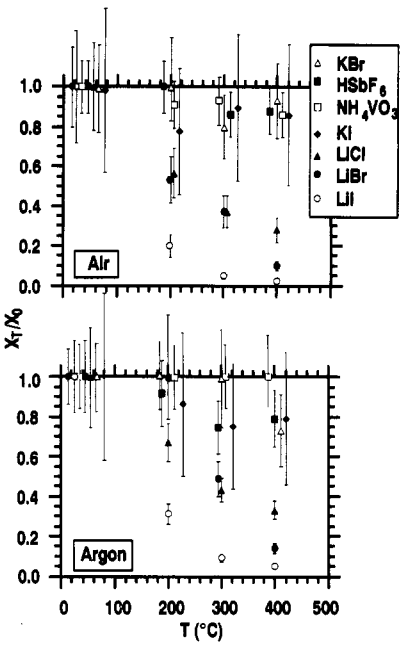

Figure 4. Plot of the relative loss of Br^- (LiBr ●, KBr Δ), I^- (LiI ○, KI ◆), Cl^- (LiCl ▲), SbF_6^- ($HSbF_6$ ■), and VO_3^- (NH_4VO_3 □) determined by RBS, as a function of temperature of thermal treatment (held at each temperature for 3 h) under air and under argon. The points are shown displaced from the nominal temperatures to avoid overlap.

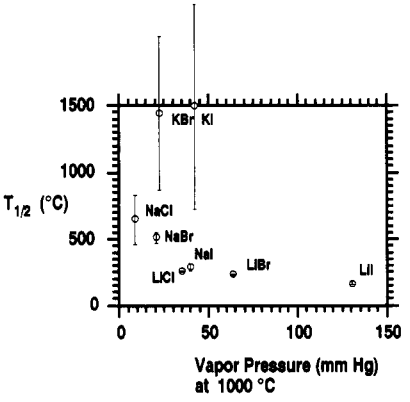

Figure 5. Plot of the estimated temperature at which half of the halide would be lost ($T_{1/2}$, °C) following the protocol in the research versus the vapor pressure of the salt at 1000 °C. The error bars represent error in the calculation of the least-squares line for each salt.

conditions in air ($T_{1/2}$, °C) versus the vapor pressure of the salt at 1000 °C calculated from literature values.[10] The value of $T_{1/2}$ was estimated from a straight line, calculated by least-squares analysis, through the data in Figures 3 and 4. We omit data for the compounds NH_4VO_3 and $HSbF_6$ because we could find no data on their vapor pressures. The vapor pressures of the salts were calculated at 1000 °C and not at the lower temperatures of our experiments because the literature values for the temperature dependence of the vapor pressures were not valid for low temperatures (<∼1000 °C). Thus, the data in Figure 5 have no quantitative significance. They do, however, show a rough correlation between the relative rate of loss of halide and the vapor pressure of the salt.

(7) Chu, W. K.; Mayer, J. W.; Nicolet, M. A. *Backscattering Spectrometry*; Academic Press: New York, 1977.
(8) Feldman, L. C.; Mayer, J. W. *Fundamentals of Surface and Thin Film Analysis*; North-Holland: New York, 1986.
(9) *Handbook of Chemistry and Physics*, 55th ed.; Weast, R. C., Ed.; CRC Press: Cleveland, OH, 1974–1975; p B-133.

(10) The vapor pressures (mmHg) of halide salts at 1000 °C, based on calculations from literature values (*Handbook of Chemistry and Physics*, 64th ed.; Weast, R. C., Ed.; CRC Press: Cleveland, OH, 1983–1984; pp D-215–217), are LiI (131) > LiBr (64) > KI (43) > LiCl (35) ∼ NaI (40) > NaBr (21) ∼ KBr (23) > NaCl (9).

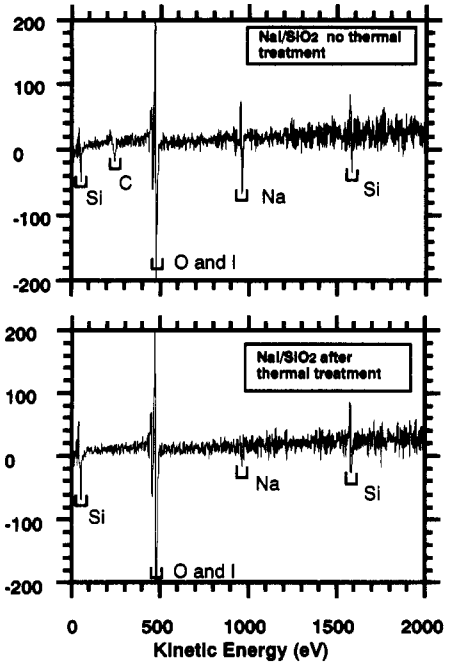

Figure 6. Plot of the derivative of the AES signal intensity versus kinetic energy (electronvolts) of the Auger transition for a NaI/SiO_2 sample before and after thermal treatment (at 200, 300, and 400 °C for 3 h each).

If the mechanism for the loss of the halide salt is the vaporization of the salt, then the cation must volatilize with the anion. Figure 6 presents the results of Auger analyses of the NaI-doped SiO_2 sample before any thermal treatment and after the series of thermal treatments in air. The samples were sputtered to remove any surface impurities and analyzed for the relative content of Na, Si, O, and I, and a survey spectra was taken. Figure 6 shows the derivatives of the Auger signal intensities from the survey spectra, which show the presence of Si, C (in the unheated sample, presumably from the presence of alkoxides in the gel), O and I (which we cannot distinguish between because the energies are too close), and Na. The normalized content of sodium, the ratio of the content of sodium to the content of silicon after thermal treatment, decreased to approximately 20% of its original content.[11] This result is consistent within experimental error with the decrease in the content of iodide, estimated by RBS to be approximately 10% under the same conditions.

Examination of the surface of the sample by AES (in the scanning mode) showed heterogeneities: precipitates rich in iodide in an iodide-poor sol–gel matrix. These precipitates (most diameters $\leq 2\ \mu M$) are small compared to the regions examined by both RBS and AES (in the analytical mode).

The data presented in this paper for NaI are compatible with, but do not demand, a mechanism for loss of halide by volatilization of NaI. Because AES is a surface-sensitive technique, it would not distinguish loss of Na^+ from the surface by volatilization, migration into the bulk, or segregation into phase-separated regions. Previous work on CsCl-doped SiO_2 revealed the loss of Cl^- without the loss of Cs^+.[12] This observation suggests loss of HX by hydrolysis of MX.

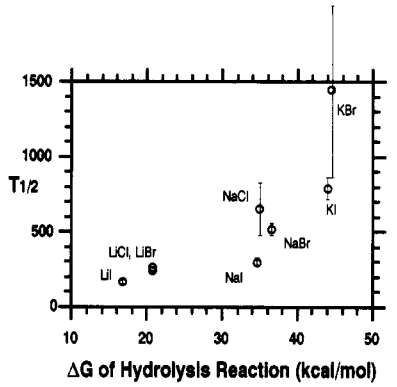

Figure 7. Plot of the estimated temperature at which half of the halide would be lost ($T_{1/2}$, °C) following the protocol in the research versus the ΔG of formation of the hydrogen halide.[12] The error bars represent error in the calculation of the least-squares line for each salt.

Figure 7 presents a plot of $T_{1/2}$ versus the ΔG for formation of HX by reaction of MX with water (eqs 5 and 6), calculated from literature values.[12] These data show

$$MX_c + H_2O_l \rightarrow HX_v + MOH_c \quad (5)$$

$$\Delta G_{HX} = \Delta G_{HX_v} + \Delta G_{MOH_c} - \Delta G_{MX_c} - \Delta G_{H_2O_l} \quad (6)$$

a rough correlation between the values of ΔG for the free energy of formation of the hydrogen halide and the rate of loss of the halide from the silicate matrix.

Conclusions

The depth profile of iodide as a function of temperature in Figure 2 shows an uneven distribution of iodide in the sample after treatments at $T = 200$ °C/3 h. The composition of the iodide is lower near the surface than near the silicon substrate. This observation suggests that mass transport—either of the salt diffusing out of the sample or of a reagent (O_2, H_2O) diffusing into the sample—may be significant under these conditions. At higher temperatures, there is little evidence for a concentration gradient in the sample. The thicknesses of the coatings of other samples were too narrow to distinguish whether a concentration gradient existed in these samples.

The difference in the rate of loss of halide under air or argon atmospheres is small enough to be of only marginal significance. The observation that the rate of loss is the same in oxidizing and nonoxidizing environments is inconsistent with oxidation as a step in the mechanism for the loss of halide. The relative rate of loss of the halides correlates roughly with the vapor pressures of halide salts (Figure 5)[10] and with the ΔG of formation of the hydrogen halides from metal halide and water (Figure 7).[13] These observations suggest that the loss of halide proceeds by volatilization of the metal halide itself and/or by hydrolysis of the metal halide to the hydrogen halide. The rate of diffusion of the volatile species from the gel matrix may contribute to the overall rate under some conditions.

The decrease in the relative content of sodium, as measured by AES, after thermal treatment is consistent with volatilization of sodium iodide as one mechanism of

(11) Powell, C. J.; Seah, M. P. *J. Vac. Sci. Technol. A* **1990**, *8*, 735–763.

(12) After initial heating of the sample to 300 °C, the signal due to chloride in the RBS profile decreased to 40 mol % relative to cesium; by 700 °C, it was less than 10%. This observation indicated that chloride ion had volatilized, probably as HCl (Schutte, C. L.; Whitesides, G. M. *Chem. Mater.* **1990**, *2*, 576.

(13) The ΔG of formation of hydrogen halide from the metal halide, based on calculations from literature values (*Handbook of Chemistry and Physics*, 64th ed.; Weast, R. C., Ed.; CRC Press: Cleveland, OH, 1983–1984; pp D-50–93) and using crystalline metal halide, crystalline metal hydroxides, gaseous hydrogen halides, and liquid water as the standard states. These values are LiI (16.78) < LiBr (20.79) ~ LiCl (20.87) < NaI (34.76) ~ NaCl (35.04) ~ NaBr (36.67) < KI (44.14) ~ KBr (44.34) in units of kcal/mol at 25 °C.

loss but is subject to other interpretations. It was not possible to measure the concentration of this ion in the bulk sample, since AES is a surface-sensitive technique and RBS cannot distinguish sodium ion against a silicon background. The observed loss of sodium may thus represent either volatilization of NaX or migration of sodium ion away form the surface and into the bulk of the silica or into precipitates of iodide-rich material. In the case of a similar gel containing CsCl[12], the chloride clearly volatilized independently of the cesium ion, which remained in the gel.

Acknowledgment. We are grateful to Professor Greg Ferguson (Lehigh Unviersity) for valuable discussions. C.L.S. acknowledges financial support from the American Association of University Women through a Dissertation Fellowship (1988–1989). John Chervinski, of the Division of Applied Sciences, Harvard University, was very helpful in assisting with the RBS measurements. E. L. Shaw, MIT, performed the Auger analyses.

Laser-Assisted Vacuum Deposition of 10-(1-Pyrenyl)decanoic Acid: In Situ Fluorescence Observation of the Process

Akira Itaya,* Satoru Takada, and Hiroshi Masuhara*

Department of Polymer Science and Engineering, Kyoto Institute of Technology, Matsugasaki, Kyoto 606, Japan

Received July 11, 1990. Revised Manuscript Received December 21, 1990

Laser irradiation effects on the deposition process (laser-assisted deposition) of 10-(1-pyrenyl)decanoic acid (PyC_{10}) were investigated by measuring in situ fluorescence spectra during deposition. Fluorescence spectra of films prepared by laser-assisted deposition were different from those of normally deposited films and depended upon laser fluence. A difference in the absorption spectrum among these films was also observed. Laser irradiation effects on normally deposited films of PyC_{10} (irradiation after deposition) were investigated for comparison. On the basis of these results, the high potential of laser-assisted vacuum deposition is discussed.

Introduction

Important factors that determine the vacuum-deposition process for organic compounds are both interaction among deposited molecules and interaction between the molecules and substrate surface. Substrate temperature, deposition rate, and surface property of substrates were examined as a parameter that determines the formation mechanism of organic deposited films. In the case of epitaxial growth of semiconductor films, recently the effect of the light irradiation on the surface-growing process has been studied as a new parameter.[1,2] The light- or laser-assisted epitaxy has induced a change of morphology, an increase in growth rate, and so on. Thus, it is of interest to investigate a light irradiation effect during deposition of organic compounds, in particular, organic compounds containing π-electronic groups. For example, it has been reported that UV-light-assisted vacuum deposition of spiropyran compounds gave a 100% amorphous film and that reversible photochromism was observed in the deposited film.[3]

Recently, we prepared vacuum-deposited films of ω-(1-pyrenyl)alkanoic acids (PyC_n, where n represents the number of methylenes in the substitution), a type of pyrene derivative, and studied on their fluorescence properties in connection with the deposition mechanism and the resulting chromophore association in the film.[4-7] We also reported interesting phenomena of fluorescence spectral changes of these deposited films caused by irradiation with an excimer laser.[8] This spectral change was caused by a nonlinear photochemical process with respect to irradiation intensity. A similar phenomenon was also observed for cast films of PyC_n and for Langmuir–Blodgett (LB) films of a mixture of PyC_n and arachidic acid.[9,10] Thus, we found that a thermalization process from higher excited singlet states of pyrenyl chromophores is responsible for the fluorescence spectral change induced by excimer laser irradiation and leads to a common local structure among cast, vacuum-deposited, and LB films.[10]

Furthermore, we applied the fluorescence spectroscopic method to in situ observation of the vacuum-deposition process of 10-(1-pyrenyl)decanoic acid (PyC_{10}) and discussed the formation mechanism of excimer sites in deposited films on the basis of the observed thickness-dependent fluorescence spectra.[11] Thus, the fluorescence spectroscopy was shown to be an effective and powerful method for elucidating the formation process of vacuum-deposited film, as was an investigation on the formation process of monolayers on water subphase.[12]

Pyrene is one of the representative compounds of which photophysical data are well documented.[13] The fluores-

(1) Yokoyama, H. *Appl. Phys. Lett.* **1986**, *49*, 1354.
(2) Matsumura, N.; Fukada, T.; Saraie, J. *J. Cryst. Growth* **1990**, *101*, 66.
(3) Yoshida, T.; Morinaka, A.; Funakoshi, N. *Thin Solid Films* **1988**, *162*, 343.
(4) Mitsuya, M.; Taniguchi, Y.; Tamai, N.; Yamazaki, I.; Masuhara, H. *Thin Solid Films* **1985**, *129*, 245.
(5) Taniguchi, Y.; Mitsuya, M.; Tamai, N.; Yamazaki, I.; Masuhara, H. *Chem. Phys. Lett.* **1986**, *132*, 516.
(6) Itaya, A.; Kawamura, T.; Masuhara, H.; Taniguchi, Y.; Mitsuya, M.; Uraki, H.; Kano, K.; Hashimoto, S. *Chem. Lett.* **1986**, 1541.
(7) Mitsuya, M.; Kiguchi, M.; Taniguchi, Y.; Masuhara, H. *Thin Solid Films* **1989**, *169*, 323.
(8) Itaya, A.; Kawamura, T.; Masuhara, H.; Taniguchi, Y.; Mitsuya, M. *Chem. Phys. Lett.* **1987**, *133*, 235.
(9) Itaya, A.; Kawamura, T.; Masuhara, H.; Taniguchi, Y. *Thin Solid Films* **1990**, *185*, 307.
(10) Itaya, A.; Masuhara, H.; Taniguchi, Y.; Imazeki, S. *Langmuir* **1989**, *5*, 1407.
(11) Itaya, A.; Takada, S.; Masuhara, H.; Taniguchi, Y. *Thin Solid Films*, in press.
(12) For example: Chauvet, J.-P.; Agrawal, M.; Patterson, L. K. *J. Phys. Chem.* **1988**, *92*, 4218.

0897-4756/91/2803-0271$02.50/0